Turbulence characterization at tidal-stream energy site in Alderney Race

A. Sentchev
Univ. Littoral Côte d'Opale, Univ. Lille, CNRS, UMR 8187, LOG, Laboratoire d'Océanologie et de Géosciences, F-62930 Wimereux, France

M. Thiébaut
France Énergies Marines, Technopôle Brest-Iroise, 525 Avenue Alexis de Rochon, 29280 Plouzané, France

S. Guillou
Normandie Univ, UNICAEN, Laboratoire Universitaire des Sciences Appliquées de Cherbourg, LUSAC, EA4253, F-50130 Cherbourg-Octeville, France

ABSTRACT: Alderney Race, located between the Alderney Island (UK) and Cotentin Peninsular (France), is a site with high tidal-stream energy potential. Circulation through Alderney Race is complex, largely dominated by tides with current speed exceeding 5 m/s at spring tide. Current velocity measurements from two bottom-mounted ADCP are used to assess the variability of velocity and turbulence in the water column. Using the velocity profiles recorded by ADCPs at 2 Hz, the time variability of the flow and turbulence was quantified with respect to tidal conditions. Turbulence metrics such as the dissipation rate (ε) of turbulence kinetic energy and the integral lengthscale (L) were estimated through the spectral approach and used in analysis of temporal variability of turbulent motions. Turtulence intensity (I) was also estimated and compared to scaling properties of turbulence. The mooring locations match areas with very different turbulence regime. This difference is found to be related to large scale bathymetry features which modify the velocity profile shape and turbulence. All turbulence parameters were found larger at the northern ADCP site where current velocity is larger. This high level of turbulence is assumed to be caused by the current interaction with irregularities of bathymetry and enhanced friction. At the southern ADCP location, over relatively smooth bathymetry, the variability of turbulence was found much smaller and to be depended on the velocity shear. These results highlight large spatial variability in turbulence characteristics occurring at rather short distance within the prospective site. The results could provide advanced information to turbine developers.

1 INTRODUCTION

In recent years, tidal energy sector has been growing rapidly in interest as more countries look for ways to generate electricity without relying on fossil fuels. In comparison to other sources of renewable energy, tidal-stream energy has many perceived benefits, including the quality of electricity production because of its predictability (e.g. Lewis et al. 2019) and the social acceptance level due to a reduced visual impact. The majority of TECs are designed to be located in the bottom boundary layer, a region where the flow experiences friction from the seabed. Due to friction effect the current velocity profile in the lower layer has a non-linear shape. The 1/7th power law approximation is typically used to characterize the velocity profile in a flow and resource assessment at tidal-stream energy sites (e.g. Batten et al. 2008, Gooch et al. 2009, Thiebaut & Sentchev 2017). However, a number of factors, including the acceleration/deceleration of the tidal flow, wave-current interaction, seabed forms, etc., can cause deviations from the 1/7th power law formulation.

Two national research programs (Thymote and Hyd2M), funded by the French Research Agency French (ANR) and by FEM, and focusing on assessment of tidal stream variability in Alderney Race, wave-current interaction, and turbulence, provided a large quantity of data and model simulation results in Alderney Race (e.g. Bennis et al. 2020; Thiebaut et al., 2020a,b). In the UK, similar investigation at the European Marine Energy Centre site (EMEC) has been conducted (e.g. Brian G. Sellar et al., Energies 2018; Osalusi et al., 2009; Hay et al., 2013).

Towed ADCP surveys performed in Alderney Race recently in the frame of Hyd2M program revealed spatial variability of the velocity profile shape as large as temporal variability (Sentchev et al. 2020a, Thiebaut et al. 2019). The northern sector of Alderney Race experiences this particularly large variability which was found to result from the tidal flow interaction with bathymetric constrictions.

It was assumed that the seabed topography, with depth decreasing by more than 20 m over a short distance (~1 km) and nature of sediments (Furgerot et al., 2019), generates enhanced turbulent motions and mixing which could modify the velocity profile shape (e.g. Ikhennicheu, et al., 2019). Based on the data from the towed ADCP survey, a comprehensive analysis of the tidal current structure in the whole water column was done (Sentchev et al. 2020a).

In the present study, we decided to go further and to investigate the flow characteristics in the lower layer, experiencing the effect of friction. High quality velocity measurements from two moorings were used. We perform an estimation of scaling parameters of turbulence generated by bottom friction. We attempt to relate these turbulence metrics to some basic parameters of the tidal flow, the velocity profile shape and mean shear, and we assess the temporal evolution of all quantities. This allows to recognize what parameters of the mean flow are suitable for turbulence quantification. We also assess the spatial variability of turbulence parameters. The results are assumed to be useful for tidal stream turbine developers.

2 DATA AND METHODS OF ANALYSIS

2.1 *Study site and velocity measurements*

Velocity measurements were performed in the eastern (French) sector of Alderney Race, northwest of the Cotentin Peninsula (Fig. 1). The water depth is less than 40 m in the majority of the domain with an abrupt increase of depth, to more than 60 m, in the northern part (Fig. 1). This large fall of water depth is the major feature of local bathymetry. Another interesting feature, closely associated to the first one, is the spatial variation in nature of the seabed, which has been documented in detail by Furgerot et al. (2019). The sea surface height (SSH) exhibits a wide range of variations (2.5-7 m) predominantly semi-diurnal and globally symmetric. Current velocities, on average, are slightly higher during ebb tide than during flood tide. However the largest current speed location varies with respect to tidal conditions. Peak flood and ebb tidal velocities occur at high and low water respectively, and the current reversal occurs at mid-tide. Thus, the tidal current dynamics in Alderney Race is an example of the progressive wave system. Depth-averaged peak ebb flow field from the local model simulations is given in Figure 1 (see Bailly du Bois et al. 2012 for details of the model). The maximum current speed is observed at a distance of ~5 km west of the Cotentin coast, in the area where the depth is less than 30 m.

Static point velocity data were collected at two locations (Fig. 1) matching very different hydrodynamic conditions and seabed topography. At the southern location (site A), the seabed topography is relatively smooth with a majority of cobbles and blocks and possible corestones (Furgerot et al., 2019). Peak tidal current velocity, after depth averaging, varies in the range 1.5-2.8 m/s with respect to tidal conditions. The velocity measurements were performed during four months, starting from March 2018, with an upward-looking 500 kHz broadband Teledyne ADCP V50. The data acquired during two days (28-29 June 2018) were used in this study. This was spring tide period characterized by largest current velocities and also calm weather conditions: the significant wave height was less than 0.7 m. ADCP was mounted on the OPENHYDRO experimental platform sitting motionlessly on the seabed with depth 34 m at low tide. The profiling range was from 2 to 29 m above the seabed with 1-m vertical spacing. Velocity values in the surface 5 m thick layer were not considered in analysis. Velocity profiles at one-hour resolution were derived from ADCP measurements performed at 2 Hz during 20-minute bursts within each hour.

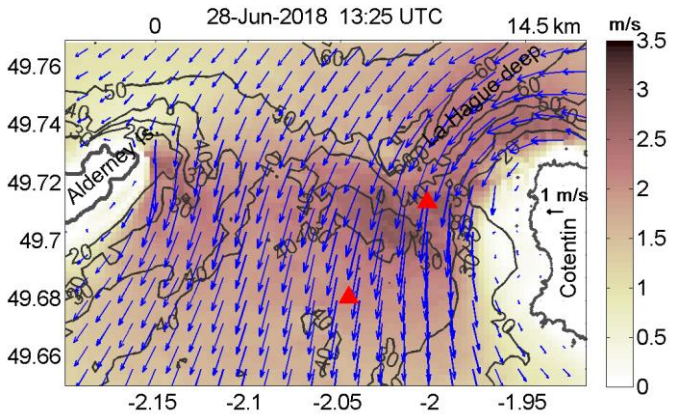

Figure 1. Depth-averaged current velocity field in Alderney Race on ebb tide from model results (Bailly du Bois et al. 2012). Triangles show the location of bottom-mounted ADCPs. Geographic names used in the text are also shown. Bathymetry contours (20, 30, 40, 50, 60 m) are given in black. High resolution bathymetry map is given in (Furgerot et al. 2019).

At the northern location (site B), two upward-looking RDI Workhorse 600 kHz four-beam ADCPs were deployed simultaneously on the seafloor (31 m mean water depth) approximately 4 km offshore. ADCPs operated in master-slave configuration with eight beams enabling to resolve six components of the Reynolds stress tensor (see Thiebaut et al., 2020a for more details). The instruments were mounted on a specifically designed frame having the following features: 3.3 m long, 2.5 m wide and 2 100 kg weight. The ADCPs recorded velocities at 2 Hz with 1.3 m vertical resolution (bin size), starting 2.2 m from the seafloor (the first bin). The measurements lasted 38 days, from September 27 to November 03, 2017. Only the data recorded between November 01, 2017 - 01:45 UTC and November 02, 2017 - 13:45 UTC were selected for subsequent analysis of turbulence using the spectral approach. During this 36-

hour long period, the depth averaged flow speed reached 3.5 m/s and the wave forcing was the weakest: waves with significant wave height 0.6 m and period 6 s were observed. It was found that during this calm period, the contribution of waves to velocity variance became insignificant at depth greater than 10 m (Thiebaut et al., 2020a). For this reason, only velocities in the range from 2 to 20 m above bottom (mab) were considered.

The most prominent feature of this measurement site is large bathymetry gradients observed northward. The seabed decreases rapidly from 30 m to 60 m over a short distance, less than 2 km. Coarse sediments (cobbles, boulders, dropstones) cover the seabed at the site (Furgerot et al., 2019) and create larger roughness. As documented in recent studies (e.g. Bailly de Bois et al. 2012, Sentchev et al. 2020a), the La Hague deep (Fig. 1) plays an important role in local hydrodynamics by constraining the current direction and generating large turbulence which affects the velocity distribution throughout the water column.

2.2 *Data analysis and turbulence characterization*

Horizontal velocity components recorded by ADCP were projected on along- and cross-stream axes (x and y respectively) of the tidal current ellipse. The projection angle (20° clockwise at site A and 25° at site B) matches the orientation of the tidal current ellipse with respect to North in the lower layer of the water column 20-m thick. Time series of the streamwise velocity component, referred to as U_x, and spanwise velocity (U_y component), were thus generated for further analysis.

Standard statistical parameters were estimated using the velocity time series provided by ADCP: the time mean, the maximum and the standard deviation of velocity variations. The turbulence intensity, often referred to as turbulence level, is defined as:

$$I = \frac{\sqrt{\sigma^2 - \sigma_N^2}}{U},$$

where U is the mean flow speed estimated from three mean velocity components (streamwise U_x, spanwise U_y and upward U_z) as

$$U \equiv \sqrt{U_x^2 + U_y^2 + U_z^2}, \text{ and } \sigma \equiv \sqrt{\frac{1}{3}\left(\sigma_x^2 + \sigma_y^2 + \sigma_z^2\right)}$$

is the standard deviation from the mean velocity, and σ_N^2 is the variance of velocity measurements induced by Doppler noise. The latter was estimated from the power spectra density (PSD) of velocity components at different depth levels according to (McMillan et al. 2017).

The dissipation rate, ε, of the turbulent kinetic energy was also estimated from the PSD of velocity, $E(k)$, assuming the Kolmogorov relationship of the local isotropic turbulence (Pope, 2000):

$$E(k) = C\varepsilon^{2/3}k^{-5/3},$$

where C is the Kolmogorov's constant (C = 1.5) and k is the wavenumber. Using Taylor's assumption of frozen turbulence, the frequency f and wavenumber k can be related to the mean velocity U such as: $k = 2\pi f / U$. Thus, the dissipation rate can be estimated from the power spectrum as (Thomson et al. 2012):

$$\varepsilon = \left(\frac{C_0}{C}\right)^{3/2}\left(\frac{2\pi}{U}\right)^{5/2}$$

where C_0 accounts for the height of the PSD slope which best fits the spectrum in the inertial subrange.

The value of ε is used to estimate another important scaling property: the integral lengthscale L, thought as the size of the most energetic turbulent eddies, defined by (Pope, 2000):

$$L = \frac{\sigma_u^3}{\varepsilon}$$

To characterize the mean tidal flow, one hour averaged velocity profiles in the lower layer of the water column (2 – 20.4 mab) were approximated by a power law

$$U(z) = \bar{U}\left(\frac{z}{\beta h}\right)^{1/\alpha},$$

with bed roughness coefficient β, vertically averaged velocity $\bar{U}$, and the water column height h (21 m). The power coefficient α is defined empirically and can strongly depend on the seabed roughness and velocity range. Bed roughness coefficient β is related directly to grain size of seabed sediments and can vary in a large range. This formulation, proposed by Soulsby (1997) on the basis of experiments in flume tank and *in situ* measurements, is adopted by the tidal energy community for characterizing the technically exploitable resource at prospective sites (e.g. Myers and Bahaj 2009, Lewis et al. 2017, Thiebaut & Sentchev, 2017). The fitting of velocity profiles to the power law is performed in a least-squares sense after linearizing the equation by log function. The resulting power law coefficient α provides the minimum approximation error for a given value of β, which was also varied iteratively in the range 0.05 to 0.5.

3 RESULTS

The tidal stream and turbulence were assessed first using the data from the southern ADCP mooring (site A) and the results are compared to that from the mooring at site B, where the flow conditions are rougher. Periods used in comparison (28-29 June, 2018 and 1-2 Nov, 2017) are characterized by low

wave forcing thus allowing an accurate estimation of the scaling properties of the bottom friction generated turbulence. Two-dimensional spectrum of current velocities on peak flood flow (Fig. 2) reveals that the contribution of waves to energy spectrum becomes visible for frequencies less than 0.1 Hz. Above this frequency, the level of velocity variations in the upper layer is notably lower than in the lower half of the water column. This confirms a limited contribution of orbital velocities of wind waves to the overall velocity variance. Time series of significant wave heights (H_s) also demonstrated low values of H_s at periods lower than 10 s for this period of observations. Thus the frequency 0.1 Hz is adopted as the lower limit of the inertial subrange spanning up to 0.5 Hz.

Figure 3 shows PSD distribution of the streamwise velocity component U_x on flood and ebb tide at different depth levels. Spectral analysis of velocity time series clearly demonstrates a locally isotropic turbulence in a range of depths from 5 to 16 mab. The spectral slope of PSD distribution varies from -1.65 to -1.70 at these depth levels (Fig. 3), and the ratio of standard deviations σ_Y / σ_X and σ_Z / σ_X are 0.96 and 0.30 respectively. Despite large difference in ratios, the mean spectral power level for all three velocity components appeared very close in the inertial subrange, thus supporting the hypothesis of isotropic turbulence. The turbulent kinetic energy of the flow is cascading from larger eddies of size L to smaller eddies of size less than one mm and then dissipates into heat. It appears convenient to perform estimation of the major turbulence metrics within this layer (5- 16 mab) – also corresponding to the tidal turbines' hub and rotor location (e.g. Zhou et al. 2014). More upwards, from 16 to 20 mab, the spectral slope decreases to -1.46 making the estimation of the scaling properties of turbulence less reliable.

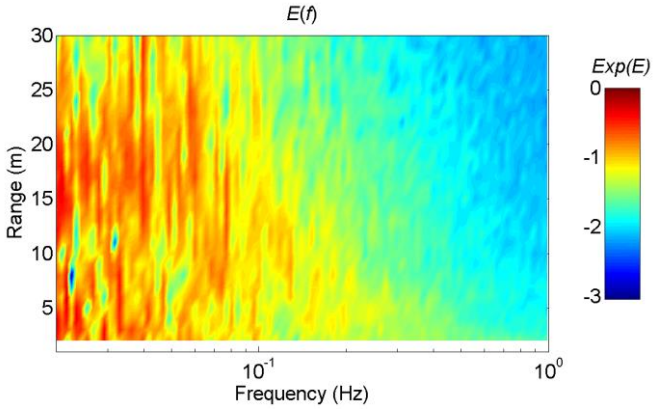

Figure 2. Power spectral density distribution at different depth levels at site A during peak flood tide on 28-Jun-2018.

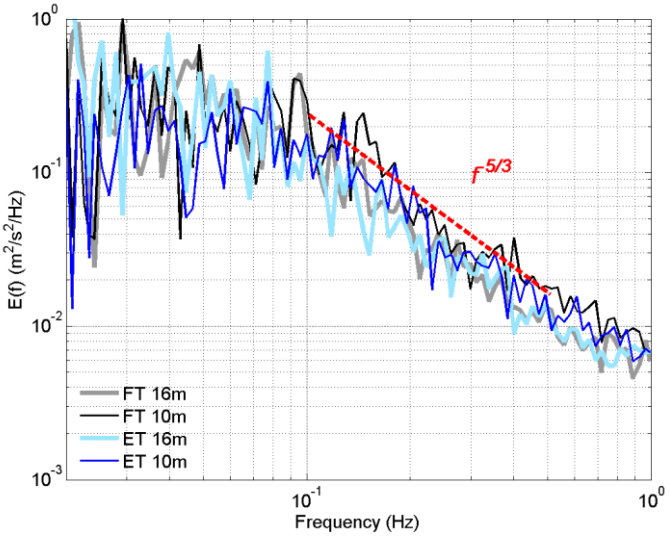

Figure 3. Power Spectral Density (PSD) of the current velocity (streamwise component) at depth levels 10 and 16 mab at site A on 28-Jun-2018. Velocity spectra during peak flood tide (FT) are shown by gray and black, and during ebb tide (ET) by light and dark blue. Red dashed line shows the spectral slope $f^{-5/3}$ in the inertial subrange.

Velocity profiles during the peak ebb and flood flows (U_x component) look different (Fig. 4). The major difference is observed in the lower layer where the profile appears more sheared on ebb tide and homogeneous on flood tide. Profile approximation by a power law provides the exponents 1/5 and 1/7 for peak ebb of flood tide conditions respectively. Figure 4 shows that the shape of profiles during two other hours of tidal cycle (one hour preceding and following the peak current) is similar to that of peak current. The resulting values of the power law exponent change insignificantly (± 1). The question arising from this observation is how the turbulence is affected by the difference in profile shape between ebb and flood flow? For clarity, we restrict the analysis by considering the peak current period on ebb and flood tide. Three tidal cycles under calm weather conditions were used in analysis.

Table 1 summarizes the scaling properties of turbulence for both tidal stages and also gives the turbulent intensity values. Most of similarity in turbulence regime is observed at 10 mab –at typical hub height. The level of the ambient turbulence (I) is close to 10%, the dissipation rate of TKE (ε) is within the range 2 – 2.6 x 10^{-3} m^2s^{-3}. The size of the energy containing eddies is also similar (~7.5 m). At range 16 mab (i.d. above hub height), the difference affects only two quantities – ε and L. The analysis reveals larger size of eddies and lower dissipation rate on ebb flow.

The major difference in turbulent parameters is found below the hub height, at 5 mab. Here, the size of energy containing eddies is four times larger on ebb tide than on flood tide. This is the direct consequences of the velocity shear which is 40% larger on ebb tide (mean shear 0.07 s^{-1}). The level of ambient

turbulence I is also larger on ebb tide (16%) compared to I on flood tide (13%). But this difference can be explained by lower velocity on ebbing tide which increases artificially the ratio σ/U. The integral lengthscale L appears to be relevant for characterizing the change in turbulent regime of the flow. The small size of turbulent eddies on flood flow is a consequence of mixing which breaks down large eddies. The shape of velocity profiles, characterized by a power law exponent is another metric useful for turbulence characterization. Therefore, sheared profiles correspond to a different spatial structure of turbulence, with larger size eddies which can interact with an operating tidal turbine in a different way.

To verify the relationship between the velocity shear and turbulence, we analyzed the flow regime and turbulent quantities at site B, located 4 km northward. Velocity profiles at 1-hour resolution reveal more powerful tidal stream with velocities up to 3.4 m/s in the upper layer (Fig. 5). They also show a significant difference in shape, already revealed for site A: more homogeneous profile on flood flow and sheared on ebb flow with power law exponent 1/6 and 1/4 respectively. The optimal bed roughness coefficient value was found to be 0.45 (corresponding to 0.45 10^{-3} m). Scaling properties of turbulence are given in Table 1 (site B). They evidence that, in the sheared velocity layer on ebb tide, the integral lengthscale is larger and the dissipation rate is smaller. On the contrary, the level of ambient turbulence, quantified by I is very similar (18%).

Table 1. Turbulence properties of the tidal flow during peak flood and ebb tide conditions at sites A and B: dissipation rate ε of the turbulence kinetic energy, integral lengthscale L, and turbulence intensity I.

Dist. from bottom	ε(m^2s^{-3})	L(m)	I(%)
Site A			
	Ebb tide		
16 m	1.1×10^{-3}	12.9	9
10 m	2.6×10^{-3}	7.5	11
5 m	6.4×10^{-3}	5.4	17
	Flood tide		
16 m	1.5×10^{-3}	7.0	8
10 m	2.0×10^{-3}	7.8	10
5 m	12.0×10^{-3}	1.5	13
Site B			
	Ebb tide		
16 m	2.6×10^{-3}	26.6	10
10 m	3.3×10^{-3}	27.3	15
5 m	4.7×10^{-3}	25.8	18
	Flood tide		
16 m	3.4×10^{-3}	30.0	14
10 m	3.9×10^{-3}	26.5	15
5 m	6.0×10^{-3}	22.4	18

In the upper half of the water column (at range more than 10 mab) both the integral scale L and dissipation are found larger on flood flow. They appear to correlate with turbulence intensity, also larger on flood tide. However the difference in I between ebb and flood flow is found very large at range 16-20 mab (Fig. 5). This is due to larger velocity variance on flood tide in the whole water column. We assume that this enhanced variability of U_x is caused by seabed irregularities upstream of the measurement site. Figure 1 shows the existence of a promontory at short distance southward of the mooring location. Note also that temporal variability of I was fond not large when considering individually ebb or flood flow stage. Hourly profiles of I appear to be similar and the range of variability is limited to 3% in the bottom layer at site B (Fig. 5).

Comparison of turbulence metrics at two sites demonstrates higher turbulence level at site B on average, with larger values of the dissipation rate ε and the integral lengthscale L caused by the flow conditions and not only by higher current speed. Large bathymetry gradients, observed northward and southward of the mooring location B, and enhanced friction, result in higher level of turbulence there. At the same time, the turbulence intensity I, in the upper layer (10-20 mab), is similar at both sites (ebb tide conditions at site B) and does not match the difference in turbulence characteristics between sites. This comparison reveals that the turbulence intensity alone does not capture quantitative changes in the turbulent regime. Others quantities, such as dissipation rate, ε, the integral length-scale, L, appear more appropriate for turbulence characterization.

4 DISCUSSION

Velocity time series used in this study were acquired as a part of two large observation programs (Thymote and Hyd2M) focusing on assessment of the tidal stream variability and turbulence in Alderney Race. The study site is a prospective tidal power site suitable for a massive deployment of tidal energy convertors (TECs) there. To be economically feasible, TECs require large current velocities: typically, spring tide velocities in excess of 2.5 m/s (Lewis et al. 2015). This condition is met over a large area within Alderney Race. As the majority of TECs are designed to be located in the bottom boundary layer, a region where the flow experiences friction from the seabed, the knowledge of vertical shear of current velocity is a major consideration. It is assumed to have important implications for turbine efficiency and resilience (e.g. Liu et al. 2012, Milne et al. 2016), for assessing the effect of turbulence (e.g. Blackmore et al. 2016), as well as for the instantaneous power available, as described in (Lewis et al.

2019). For this reason, TEC developers look for detailed characteristics of the flow speed across the area swept by the turbine blades and the velocity profile shape characterization is an important issue in the turbine performance research and in the planning stage of the projects (e.g. Tatum et al. 2016).

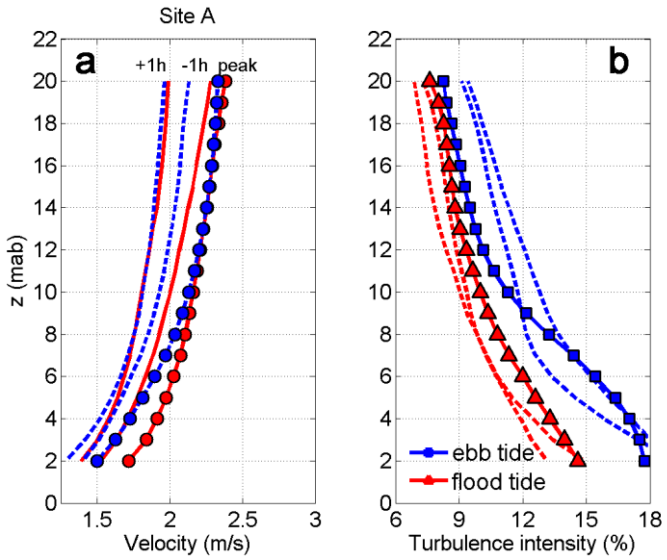

Figure 4. (a) Current velocity profiles, 1-hour averaged during three successive tidal cycles, from ADCP measurements at site A during flood tide (red) and ebb tide flow (blue). Profiles averaged over 1-hour time interval of peak ebb and flood current are shown by circles. Solid and dashed lines show average profiles for two other 1-hour time intervals: preceding and following the peak current. (b) Turbulence intensity profiles for peak ebb flow (squares) and flood flow (triangles). Profiles for peak +1h and -1h time intervals are shown by dashed lines.

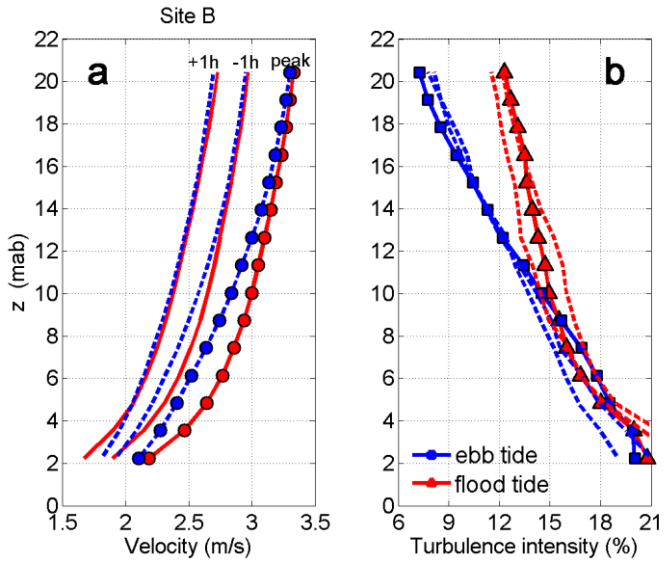

Figure 5. Same as Figure 4 but for site B.

Therefore when characterizing the velocity profile of a tidal energy site in depth-averaged model resource studies (e.g. Batten et al. 2008, Myers & Bahaj, 2010), it appears appropriate to assume a 1/7th power law, which is widely used by oceanographers (e.g. Thiebaut & Sentchev, 2017, Lewis et al. 2017). Our results revealed a deviation from the 1/7th power law. On ebb flow, the 1/5th power law was obtained, matching sheared profile, whereas on flood flow, the velocity profile is well fitted by 1/7th power law. It is worth to mention that in the tidal stream with more sheared profile (i.e. exponent 1/5) the energy resource is larger by 8% compared to flow with less sheared profile (e.g. Lewis et al. 2017). At the same time, the increase of velocity shear generates more turbulence which in turn increases unsteady loading on the blades by tidal flow instabilities (Ouro & Stoesser 2019, Gaurier et al. 2020). This is a cause of fatigue.

While the major characteristics of the mean tidal flow (speed, direction, current magnitude asymmetry, etc) are relatively simple to measure (e.g., Guerra & Thomson 2017, Thiébaut & Sentchev 2016, 2017), much less is known about turbulence. This is indicative of the inherent technical difficulties (i.e., sensor movement, limited sampling rate) in acquiring measurements of turbulent motions in fast moving currents (e.g., Milne et al. 2013).

In this study we attempted to use the conventional measurements of current velocity profiles for turbulence characterization. We also searched for metrics which are appropriate for quantification of turbulence and its potential impact on TECs.

Among different measurement techniques, employing ADV, ADCP, VMP for tidal stream and turbulence characterization at prospective tidal sites (e.g. Thomson et al. 2012, Korotenko et al. 2013 McMillan et al. 2016), ADCP is by far the instrument of choice. Deployed on bottom platforms, it provides high quality velocity time series with acquisition rate of 1 Hz, 2 Hz or even higher.

Spectral analysis of velocity time series allows estimating at least four fundamental properties of the turbulent flow: the dissipation rate of turbulence kinetic energy, ε, the integral lengthscale, L, the Kolmogorov scale, η, and the Taylor-based Reynolds number (Sentchev et al. 2020b, Thiebaut et al. 2020a). The integral lengthscale, L, provides the spatial structure of turbulence and quantifies the size of the most energy containing eddies. This quantity is useful for understanding the turbulent flow interaction with a single device (tidal turbine) or an array of devices deployed on the seabed.

The dynamics of the large-scale turbulent eddies was found sensibly different at two measurement sites, with predominantly larger turbulent motions at site B and scales comparable with the water depth. These eddies contain the largest proportion of turbulent energy, and are likely to have large effect on TECs performance. Recently, a study focusing on the assessment of the performance of a Darrieus type turbine operating in real sea conditions demonstrated that the strongest impact of turbulence on power generation by the TEC occurred when the length of the most energetic eddies matches the turbine size (Sentchev et al., 2020b).

MacEnri et al. (2013) were the first who performed a comprehensive analysis of the SeaGen performance and demonstrated that standard deviation of the velocity, assumed to be a measure of the turbulence strength, is likely to be one of the significant factors that contributes to flicker level. Large fluctuations of the output power were found at frequency ~ 0.5 Hz which is fundamental (turbine) frequency. Similar results were documented by Frost et al. (2018) for a scaled turbine, tested in the Strangford Lough (UK). Power fluctuations were related to turbulence effect.

According to our results, it is expected that in the northern part of Alderney Race, TECs will experience larger influence of turbulence with high level of fatigue caused by large size eddies. Another effect of turbulence eddies on TECs could be the enhanced fluctuations of the output power caused by turbulent eddies of size compared to a typical turbine size.

5 CONCLUSIONS

Analysis of ADCP velocity measurements in Alderney Race demonstrated large temporal variability of the velocity profile shape, in the bottom layer ~ 10-m thick, which was found correlated with the tidal conditions. At both locations, over relatively smooth bathymetry in the south and rough bathymetry in the north, ebb tide flow appeared highly sheared. Velocity profiles were accurately approximated at two sites by the power law with exponents 1/5 and 1/4 respectively on ebb tide, and 1/7 on flood tide. Large velocity shear observed in the lower part of the water column is a source of enhanced turbulence. A relationship between the dissipation rate ε, the size of energy containing eddies and the velocity shear was demonstrated. Large turbulent eddies of size comparable with the water depth were identified in the northern sector and assumed to be generated by the current interaction with a bathymetric constriction. Turbulence intensity I, is a metric that in general does not alone capture quantitative changes in the turbulent regime during the flow transition from ebbing to flooding flow or from lower to higher velocities. Other quantities, such as dissipation rate, ε, the integral lengthscale, L, appear more appropriate for turbulence characterization. The integral lengthscale is related to the spatial structure of turbulence. It is assumed to be particularly useful for TEC developers in assessing a potential interaction of the turbulent flow with turbines.

Acknowledgments

This work benefitted from the funding support from France Energies Marines and the French Government, operated by the National Research Agency under the Investments for the Future program: Reference ANR-10-IEED-0006-07 and ANR-10-IEED-0006-11. The study represents a contribution to the projects HYD2M and THYMOTE of the above program. We would like to acknowledge Lucile Furgerot (UNICAEN) for providing the data, and Anne-Claire Bennis (UNICAEN) - the head of the research project.

6 REFERENCES

Bailly du Bois, P. B., Dumas, F., Solier, L., & Voiseux, C. 2012. In-situ database toolbox for short-term dispersion model validation in macro-tidal seas, application for 2D-model. *Continental Shelf Research*, 36: 63-82.

Batten, W. M. J., Bahaj, A. S., Molland, A. F., & Chaplin, J. R. 2008. The prediction of the hydrodynamic performance of marine current turbines. *Renewable energy*, 33: 1085-1096.

Bennis, A.-C., Furgerot, L., Bailly Du Bois, P., Dumas, F., Odaka, T., Lathuilière, C. & Filipot, J.-F. 2020. Numerical modelling of three-dimensional wave-current interactions in complex environment: application to Alderney Race. *Applied Ocean Research. 95*: 102021

Blackmore T., Myers L.E. and Bahaj A.S. 2016. Effects of turbulence on tidal turbines: Implications to performance, blade loads, and condition monitoring. *International Journal of Marine Energy*. 14: 1–26

Frost, C., Benson, I., Jeffcoate, P., Elsäßer, B., & Whittaker, T. 2018. The Effect of Control Strategy on Tidal Stream Turbine Performance in Laboratory and Field Experiments. *Energies*, *11*(6) : 1533.

Furgerot, L., Poprawski, Y., Violet, M., Poizot, E., Bailly du Bois, P., Morillon, M., & Mear, Y. 2019. High-resolution bathymetry of the Alderney Race and its geological and sedimentological description (Raz Blanchard, northwest France). *Journal of Maps*, *15*: 708-718.

Gooch, S., Thomson, J., Polagye, B., & Meggitt, D. 2009. Site characterization for tidal power. *In OCEANS 2009*: 1-10.

Guerra, M., & Thomson, J. 2017. Turbulence measurements from five-beam acoustic Doppler current profilers. *Journal of Atmospheric and Oceanic Technology*, *34*(6), 1267-1284.

Hay, A. E., McMillan, J., Cheel, R., & Schillinger, D. 2013. Turbulence and drag in a high Reynolds number tidal passage targetted for in-stream tidal power. In *OCEANS 2013*: 1-10.

Ikhennicheu, M., Germain, G., Druault, P., & Gaurier, B. 2019. Experimental investigation of the turbulent wake past real seabed elements for velocity variations characterization in the water column. *Int. J. Heat and Fluid Flow*, *78*: 108426.

Korotenko, K., Sentchev, A., Schmitt, F. G., & Jouanneau, N. 2013. Variability of turbulent quantities in the tidal bottom boundary layer: Case study in the eastern English Channel. *Continental Shelf Research*, *58*: 21-31.

Lewis, M., Neill, S. P., Robins P. E., & Hashemi, M. R. 2015 Resource assessment for future generations of tidal-stream energy arrays. *Energy*, 83: 403-415.

Lewis, M., Neill, S.P., Robins, P., Hashemi, M.R., & Ward, S. 2017 Characteristics of the velocity profile at tidal-stream energy sites. *Renewable Energy*, 114: 258-272.

Lewis, M., McNaughton, J., Márquez-Dominguez, C., Todeschini, G., Togneri, M., Masters, I., Allmark, M., Stallard, T., Neill, S., Goward-Brown, A. and Robins, P. 2019 Power variability of tidal-stream energy and implications for electricity supply. *Energy*, 183: 1061-1074.

Liu, P and Veitch, B. 2012. Design and optimization for strength and integrity of tidal turbine rotor blades. *Energy*, 46: 393–404.

MacEnri J., Reed M., Thiringer T. 2013. Influence of tidal parameters on SeaGen flicker performance. *Philosophical Transactions of the Royal Society of London A: Mathematical, Physical and Engineering Sciences*, 371(1985):20120247.

McMillan, J. M., Hay, A. E., Lueck, R. G., & Wolk, F. 2016. Rates of dissipation of turbulent kinetic energy in a high Reynolds number tidal channel. *Journal of Atmospheric and Oceanic Technology*, *33*(4): 817-837.

McMillan, J. M. & Hay, A. E. 2017. Spectral and structure function estimates of turbulence dissipation rates in a high-flow tidal channel using broadband ADCPs. *Journal of Atmospheric and Oceanic Technology*, *34*(1): 5-20.

Milne, I. A., Sharma, R. N., Flay, R. G., & Bickerton, S. 2013. Characteristics of the turbulence in the flow at a tidal stream power site. *Phil. Trans. R. Soc. A*, *371*(1985): 20120196.

Milne, I. A., Day, A. H., Sharma, R. N., & Flay, R. G. J. 2016. The characterisation of the hydrodynamic loads on tidal turbines due to turbulence. *Renewable and Sustainable Energy Reviews*, *56*: 851-864.

Myers, L.E., Bahaj, A.S. 2010. Experimental analysis of the flow field around horizontal axis tidal turbines by use of scale mesh disk rotor simulators, *Ocean Eng*, 37 (2): 218-227.

Osalusi, E., Side, J., Harris, R. 2009. Structure of turbulent flow in EMEC's tidal energy test site. *Int. Communications in Heat and Mass Transfer*, *36*: 422-431.

Ouro, P., & Stoesser, T. 2019. Impact of environmental turbulence on the performance and loadings of a tidal stream turbine. *Flow, Turbulence and Combustion*, *102* : 613-639.

Pope S. B. 2000. Turbulent flows. Cambridge University Press.

Sellar, B. G., Wakelam, G., Sutherland, D. R., Ingram, D. M., Venugopal, V. (2018). Characterisation of tidal flows at the European marine energy centre in the absence of ocean waves. *Energies*, *11*: 176.

Sentchev, A., Nguyen, T.D., Furgerot, L. & Bailly du Bois, P. 2020a. Underway velocity measurements in Alderney Race: toward a 3D representation of tidal motions. *Phil. Trans. Royal Soc. A*, 2020 (in press)

Sentchev, A., Thiebaut, M. & Schmitt, F.G. 2020b. Impact of turbulence on power production by a free-stream tidal turbine in real sea conditions. Renewable Energy, 147: 1932–1940.

Soulsby R. 1997. Dynamics of Marine Sands: a Manual for Practical Applications, Thomas Telford.

Tatum, S. C., Frost, C. H., Allmark, M., O'Doherty, D. M., Mason-Jones, A., Prickett, P. W., ... & O'Doherty, T. 2016. Wave–current interaction effects on tidal stream turbine performance and loading characteristics. *International Journal of Marine Energy*, *14*: 161-179.

Thiebaut, M. & Sentchev, A. 2016. Tidal stream resource assessment in the Dover Strait (eastern English Channel). *International journal of marine energy*, 16: 262-278.

Thiebaut, M. & Sentchev, A. 2017. Asymmetry of tidal currents off the W. Brittany coast and assessment of tidal energy resource around the Ushant Island. *Renewable energy*, 105 : 735-747.

Thiebaut, M., Filipot, J. F., Maisondieu, C., Damblans, G., Duarte, R., Droniou, E., ... & Guillou, S. 2020a. A comprehensive assessment of turbulence at a tidal-stream energy site influenced by wind-generated ocean waves. *Energy*, *191*: 116550.

Thiebaut M., Sentchev, A. & Bailly du Bois *P*. 2020b. Merging velocity measurements and modeling to improve understanding of tidal stream resource in Alderney Race. *Energy*, 178: 460-470.

Thomson J., Polagye B., Durgesh V., Richmond M. C. 2012. Measurements of turbulence at two tidal energy sites in Puget Sound,WA. Oceanic Engineering, IEEE J. of Oceanic Engineering, 37(3):363–374.

Zhou, Z., Scuiller, F., Charpentier, J. F., Benbouzid, M., & Tang, T. 2014. An up-to-date review of large marine tidal current turbine technologies. In *2014 International Power Electronics and Application Conference and Exposition*: 480-484.